Unconventional superconductivity in ultrathin superconducting NbN films studied by scanning tunneling spectroscopy

Y. Noat,[1] V. Cherkez,[1] C. Brun,[1] T. Cren,[1] C. Carbillet,[1] F. Debontridder,[1] K. Ilin,[2] M. Siegel,[2] A. Semenov,[3] H.-W. Hübers,[3] and D. Roditchev[1]

[1]*Institut des Nanosciences de Paris, CNRS-UMR 7588, Université Pierre et Marie Curie-Paris 6 UPMC, 4 place Jussieu, 75252, Paris, France*

[2]*Institute of Micro- und Nano-electronic Systems, Karlsruhe Institute of Technology, Hertzstrasse 16, D-76187 Karlsruhe, Germany*

[3]*DLR Institute of Planetary Research, Rutherfordstrasse 2, 12489 Berlin, Germany*

(Received 29 March 2013; revised manuscript received 24 June 2013; published 3 July 2013)

Using scanning tunneling spectroscopy, we address the problem of the superconductor-insulator phase transition in homogeneously disordered ultrathin (2–15 nm) films of NbN. Samples thicker than 8 nm, for which the Ioffe-Regel parameter $k_F l \geqslant 5.6$, manifest a conventional superconductivity: a spatially homogeneous BCS-like gap, vanishing at the critical temperature, and a disordered vortex lattice in magnetic field. Upon thickness reduction, however, while $k_F l$ lowers, the STS reveals striking deviations from the BCS scenario, among which a progressive decrease of the coherence peak height and small spatial inhomogeneities. In addition, the gap below T_C develops on a spectral background, which becomes more and more "V-shaped" approaching the localization. The thinnest film (2.16 nm), while not being exactly at the superconductor-insulator transition (SIT) ($T_C \approx 0.4 T_C^{\text{bulk}}$), showed unconventional signatures such as the vanishing of the coherence peaks and the absence of vortices. This behavior suggests a weakening of long-range phase coherence, when approaching the SIT in this quasi-2D limit.

DOI: 10.1103/PhysRevB.88.014503 PACS number(s): 74.78.−w, 74.25.Uv, 74.55.+v, 74.62.En

I. INTRODUCTION

Despite numerous theoretical and experimental works,[1] the understanding of the phase transition from a superconducting (SC) to an insulating state in ultrathin films remains a very challenging problem. The structural properties of the films are known to play a key-role in determining the low-temperature electronic properties. Disordered SC thin films undergoing a superconductor-insulator transition (SIT) can be divided into two groups:[2] granular systems, described as an array of Josephson junctions,[3] and systems qualified as "homogeneous" where both amplitude and phase variations of the order parameter play an important role.[4] These two groups present significant differences in the electronic properties at low temperature. For example, in granular systems, the SC gap (Δ) and critical temperature (T_C) remain close to the bulk values on approaching the SIT.[3] On the contrary, in disordered "homogeneous" systems, T_C gradually diminishes[4] and eventually tends to vanish at the SIT.[5] Nevertheless, different behaviors were reported, first in the so-called "fermionic" scenario,[6–8] both T_C and Δ decrease when approaching SIT. While, on the contrary, in the "bosonic" scenario,[9–13] the gap Δ tends to a finite value with a pseudo-gap-like spectral signature while T_C decreases toward zero close to the SIT.[14,15]

It is worth noting that the SIT problem has important application issues, specifically in the field of single photon detectors[16] in which ultrathin SC films (usually NbN or NbTiN) are used. It has recently been discovered that the maximum detection efficiency occurs for film thicknesses close to the SIT.[17] A detailed study at a nanometer scale of the ultrathin superconducting films close to the SIT will help to understand the underlying microscopic processes that drive the transition as well as the photon absorption process by the SC condensate.

A way to get a new insight in the microscopic processes occurring at the SIT is to study the local properties of the SC condensate. Recently, two scanning tunneling microscopy and spectroscopy (STM/STS) experiments addressed this question, leading to different interpretations.[14,15]

In this work, we address the SIT problem locally in a direct STS experiment by varying the thickness of ultrathin NbN films from 15 down to 2.16 nm, the corresponding T_C varying from 15.0 to 6.7 K, and the Ioffe-Regel parameter $k_F l$ from 5.7 to below 2.6. Our data reveal profound changes in the local STS dI/dV spectra as the SIT is approached, which cannot be explained in the framework of the standard BCS theory. The amplitude of the coherence peaks diminishes and almost vanishes when $T_C \approx 0.4 T_C^{\text{bulk}}$. This feature is accompanied by a significant broadening of the tunneling density of states (DOS) and by the development of a characteristic V-shaped electronic background, extending to voltages 5–10 mV, significantly larger than Δ/e. In addition, a *shallow* pseudogap regime is observed in a very narrow temperature window just above T_C.

These features are similar to those reported for 3D-NbN films of comparable T_C and $k_F l$[18] but are in striking contrast with the recently reported large pseudogap regimes observed in TiN and InO.[14,15] Finally, while the vortices are observed in thicker films subject to magnetic field, their contrast in STS data diminishes with reducing thickness. In the 2.16 nm film, the vortices are not observed anymore, suggesting a weakening of the long-range phase coherence. Our results show evidence of unconventional signatures in the tunneling spectra of ultrathin films. It suggests that phase fluctuations may drive the insulating transition and have already measurable effects before the SIT.

II. FILM GROWTH AND ELECTRICAL PROPERTIES OF THE FILMS

In order to achieve as realistic conditions as possible, we studied ultrathin NbN films used in real photon detectors;[17] all films were grown *ex situ* on crystalline sapphire using identical growth conditions by DC reactive magnetron sputtering of a

 ©2013 American Physical Society

Nb target in a $Ar + N_2$ gas mixture. Their optical, electronic, and SC properties were extensively studied;[19] the structural characterization showed that the amorphous NbN films consist of nanocrystallites,[20] with a passivation layer 0.5–1 nm at the film surface.[19]

It has been shown in previous works[19] that the physical properties of the film evolve as its thickness is reduced. The 12-nm-thick films have a T_C about 15 K and $k_F l \approx 5.7$; these parameters hardly change down to 6-nm films for which $T_C \approx 14$ K and $k_F l \approx 5.6$. When the thickness is further reduced by two, i.e., for 3.2 nm, T_C drops to 10.7 K and $k_F l \approx 2.6$. Simultaneously, from 8 to 3.2 nm, the density of states (DOS) at the Fermi level is reduced by a factor greater than two. The carrier concentration, which is estimated assuming free-electrons expressions, is reduced typically by a factor 2 between thicker films and thinner films.

Since the films are prepared *ex situ*, there is a natural passivation layer 0.5–1 nm, presumably an oxidized layer, covering the top surface of the films.[19] We point out that our intention in this study is not to probe pure NbN films, which would require the growth in a UHV chamber coupled to a low temperature UHV STM. On the contrary, we aimed to probe the electronic properties of "real SC films"from which "real" single photon detectors are being fabricated. The estimation of the Ginzburg-Landau SC coherence lengths ξ for thicknesses between 15 and 3.2 nm yields values between 4 and 6 nm.[19] Thus we can assume that the films with a thickness smaller than 4 nm are in the two-dimensional limit with respect to superconductivity, since the order parameter is expected to be homogeneous in the direction perpendicular to the surface. Consequently, for the thinnest films, the oxide layer should be treated as belonging to the whole SC system. Furthermore, it is noticeable that for thicker films, where T_C is close to the bulk value $T_C = 15.5$ K, the passivation layer induces a negligible inverse proximity effect on SC. In addition, we have checked that a proximity effect cannot explain the features observed in the experiment. This point will be discussed in Sec. V.

In Fig. 1(a), the sheet resistance versus temperature dependence $R_{sq}(T)$ of the studied films, shows a typical SIT behavior of nongranular films: T_C lowers as the film thickness decreases. Being weak for thicker films (8 nm and more), the T_C reduction becomes significant for thinner films, reflecting the rapid suppression of T_C on approaching the SIT. Among the studied samples, the 2.16 nm one is the closest to the SIT, "sitting" on its SC side, and having $T_C \approx 0.4 T_C^{\text{bulk}}$. Thinner films (2.0 nm) show an insulating behavior at low temperature.

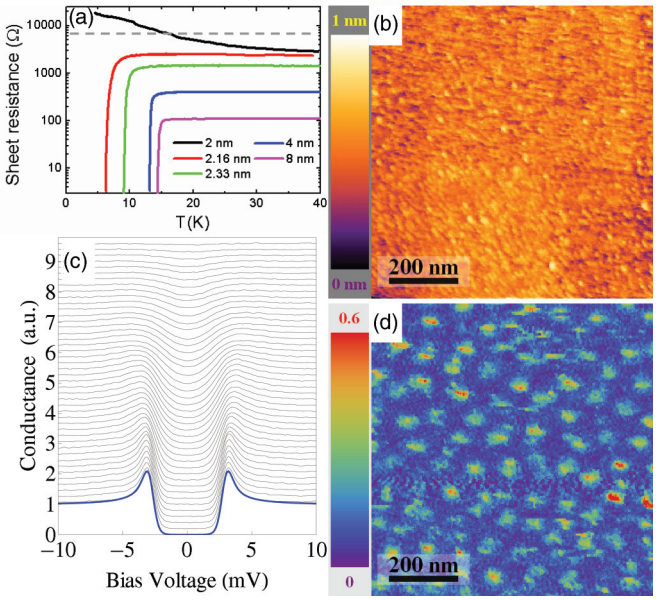

FIG. 1. (Color online) (a) Square resistivity vs temperature dependence of the studied samples; the dashed line indicates $h/4e^2$ as the quantum resistance for pairs; T_C decreases with film thickness [$T_C^{15\,\text{nm}} = 15.0$ K (not shown), $T_C^{8\,\text{nm}} = 14.5$ K, $T_C^{4\,\text{nm}} = 13.3$ K, $T_C^{2.33\,\text{nm}} = 9.4$ K, $T_C^{2.16\,\text{nm}} = 6.7$ K]. We defined T_C by the temperature reached when the resistivity equals 10% of its 40 K value. (b) Typical topographic STM image of the surface (15-nm-thick film, $T = 4.2$ K, image size; 1 μm × 1 μm). (c) Evolution of the tunneling conductance spectra (thin black lines) with temperature; bottom thick blue line: BCS fit at 2.3 K. (d) dI/dV conductance map at $V = 0$ in magnetic field ($B = 1$ T), revealing a disordered vortex lattice.

III. TUNNELING SPECTROSCOPY RESULTS

A. Evolution of the STS spectra with thickness

Constant current STM images revealed a very smooth film surface with ≈0.1 nm roughness [see Fig. 1(b)]. The measurements were performed at variable temperatures (2.3–20 K) using Pt/Ir tips. The local tunneling conductance spectra $dI/dV(V,x,y)$ were obtained by numerical derivative of raw $I(V)$ data. They are directly linked to the local quasiparticle excitation spectrum, $N_S(E,x,y)$, through the relation $dI(V)/dV \propto -\int dE N_S(E+eV,x,y)\partial f(E)/\partial E$, where $f(E)$ is the Fermi-Dirac function.

The thicker 15-nm film shows conventional and *spatially homogeneous* SC conductance spectra with a nonbroadened BCS shape, characterized by a gap $\Delta(0) = 2.85$ meV [see Fig. 1(c)]; the gap vanishes as expected for a conventional superconductor at the film T_C [extracted from $R_{sq}(T)$ measurement]. Upon application of a magnetic field, a disordered vortex lattice was revealed, attesting for local disorder existing in this extreme type II SC [see Fig. 1(d)]. These observations are in good agreement with previous reports.[18,21–23]

The evolution of the parameters as a function of the thickness, the critical temperature T_C, $k_F l$, Δ, as well as the spectral broadening Γ_{Dynes} (the two last parameters are determined by a BCS fit of a typical local spectrum), are shown in Table I for each film thickness.

TABLE I. Critical temperature T_C (extracted from transport measurements), energy gap value Δ_{BCS}, and spectral broadening parameter Γ_{Dynes} (both extracted from BCS fits of the tunnel conductance spectra), the typical spatial variation of the gap $\delta\Delta_{\text{BCS}}$ and the ratio $2\Delta_{\text{BCS}}/k_B T_C$ as a function of film thickness d.

d (nm)	15	8	4	2.33	2.16
T_C(K)	15.0	14.5	13.3	9.4	6.7
Δ_{BCS}	2.85	2.7	2.4	1.7	1.3
$\delta\Delta_{\text{BCS}}$	<0.03	0.03	0.08	0.2	...
Γ_{Dynes}	<0.01	0.01	0.01	0.05	0.1
$2\Delta_{\text{BCS}}/k_B T_C$	4.4	4.3	4.2	4.2	4.0

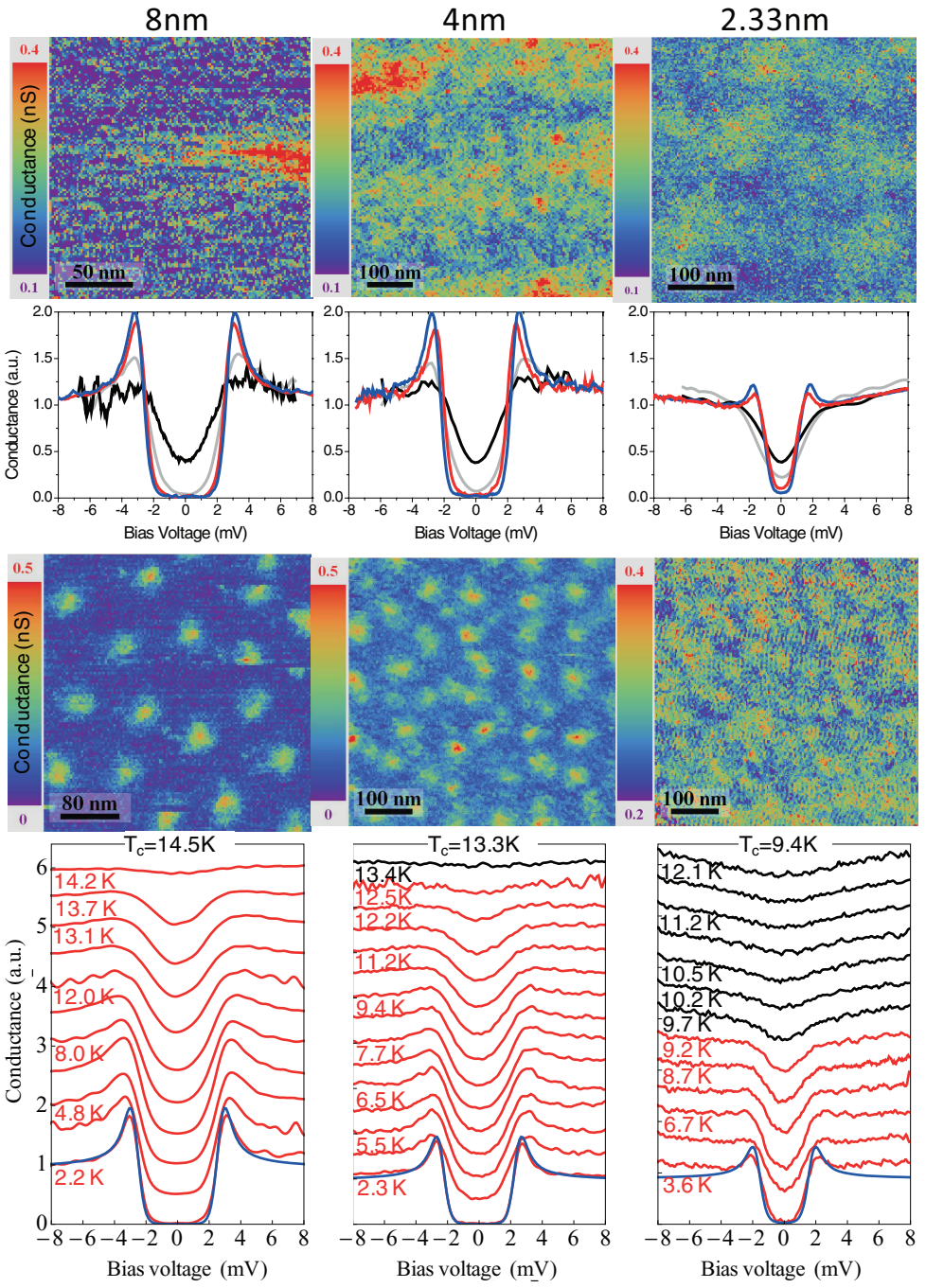

FIG. 2. (Color online) From left to right column: tunneling characteristics of 8-, 4-, and 2.33-nm-thick films. From top to bottom: the first row shows normalized STS conductance maps representing the color-coded spatial variations of the dI/dV signal measured at 2.3 K at the gap onset (for $V = 1.7$, 1.7, and 1.1 mV); second row: normalized individual tunneling conductance spectra representative of the spatial variations observed among the local conductance spectra (red and blue curves) at 2.3 K; the black curves show typical spectra measured at 4.0 K in magnetic field ($B = 1$, 1, and 2 T) at the vortex centers and outside the vortex (gray curves); third row: dI/dV conductance maps at $V = 0$ showing images of the vortex lattices at 4.0 K (for $B = 1$, $B = 1$, and 2 T); fourth row: temperature evolution of the normalized $dI/dV(V)$ tunneling spectra (vertically shifted for clarity); the temperature is indicated below the corresponding spectra. Red (black) curves correspond to the SC (normal) state. The bottom thick blue lines are BCS dI/dV calculations at the indicated temperature; an additional broadening parameter was needed to fit the data (see text).

Figure 2 summarizes STS data obtained on thinner films (8, 4, and 2.33 nm). The data are organized in three columns by thickness. From top to bottom, each column shows (i) a normalized conductance map chosen to picture out possible gap inhomogeneities, (ii) selected representative spectra, (iii) an image of the vortex lattice, and (iv) the temperature evolution of local spectra.

The 8-nm dI/dV map reveals only tiny spatial inhomogeneities of the SC gap, except in regions where structural defects occur, such as the red patch in the image. The disordered

vortex lattice is routinely observed. The temperature evolution of the tunneling spectra remains conventional, although a slight spectral broadening was detected and accounted for with a tiny Dynes pair-breaking parameter (see Ref. 24) $\Gamma_{\text{Dynes}} \approx 0.01$ meV, with a modified BCS DOS:

$$N_S(E) = \text{Re}\left[\frac{|E - i\Gamma_{\text{Dynes}}|}{\sqrt{(E - i\Gamma_{\text{Dynes}})^2 - \Delta(E)^2}}\right]. \quad (1)$$

The situation changes in the 4-nm sample. Specifically, weak spatial inhomogeneities are revealed in the tunneling conductance map, which affect the gap width and the height of the coherence peaks (see the red and blue curves below the conductance map). These inhomogeneities are characterized by two spatial length scales. The smaller one is of the order of a few nanometers, thus close to the coherence length. The larger one is of several tens of nanometers; further analysis showed that the latter originates from slight variations of the film thickness due to underlying atomic steps of the substrate. Nevertheless, the dI/dV spectra at $T \ll T_C$ remain reasonably BCS-like requiring a small spectral broadening $\Gamma_{\text{Dynes}} \approx 0.01$ meV.

In the 2.33-nm sample, the tunneling spectra undergo more pronounced changes. The conductance maps reveal inhomogeneities comparable to the 4-nm case and characterized by two length scales. While a well-defined gap in dI/dV exists everywhere, the amplitude of the coherence peaks is much reduced. The dI/dV spectra at $T \ll T_C$ are approximately described by BCS requiring a quite large spectral broadening $\Gamma_{\text{Dynes}} \approx 0.05$ meV. The peak height varies spatially at the nanometer scale (see the blue and red curves), similarly to the effects discovered in cuprates.[25] The vortex lattice is hardly observable. Note that the same qualitative behavior was observed for $B = 1$ and 3 T. Inside the cores, the spectra present a large dip with no coherence peaks. Moreover, the normal state spectra reveal a "V-shaped" background with a clear minimum at zero bias, extended over a larger energy scale than the SC gap. A shallow pseudogap (determined with respect to the superconducting critical temperature, as measured by means of transport measurement) is also observed within a 1 K range above T_C, whose energy scale is comparable to the SC gap. The spectra are poorly described by a BCS expression at $T \ll T_C$ and require $\Gamma_{\text{Dynes}} \approx 0.05$ meV.

B. Unconventional superconductivity in the thinnest 2.16-nm film

Striking changes are revealed in the tunneling characteristics of the 2.16-nm sample (see Fig. 3). The SC gap develops on a deeper V-shaped background, existing also above T_C [see Fig. 3(e)], thus characteristic of the normal state. In addition, a very shallow pseudogap seem to be present. It is important to note that it is determined with respect to the superconducting critical temperature as measured by transport measurement. Furthermore, it is difficult to distinguish it clearly from the V-shaped background. It also appears in Figs. 3(f) and 3(g) where $R_{\text{sq}}(T)$ and $dI/dV(V = 0, T)$ are presented for 2.16–8-nm films. The opening of the SC gap occurs at T_C, as it is unambiguously detected as a kink in the $dI/dV(V = 0, T)$ curves (pointed by the arrows), in contrast to the smoother

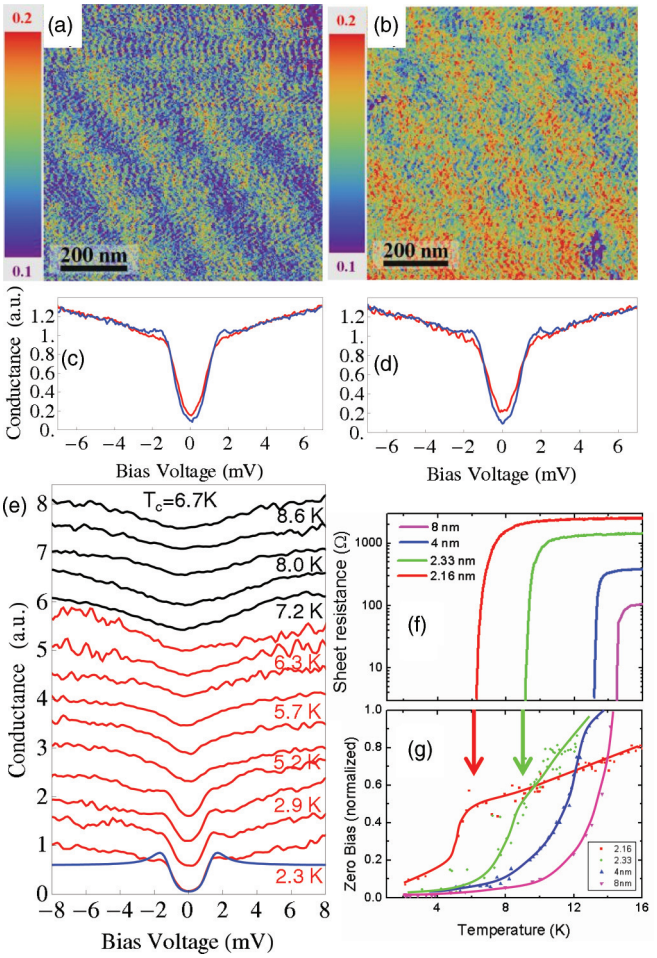

FIG. 3. (Color online) Tunneling characteristics of the 2.16-nm-thick film at 2.3 K. Zero-bias STS conductance maps at (a) $B = 0$ and (b) 3 T. Typical variations among the corresponding local spectra for (c) $B = 0$ and (d) 3 T. (e) Evolution of the $dI/dV(V)$ spectra with temperature. The bottom thick blue line is a BCS calculation at 2.3 K with an additional broadening parameter (see text). (f) Zoom on $R(T)$ of the 2.16–8-nm films compared to their (g) temperature dependence of the zero-bias tunneling conductance $dI(V = 0)/dV$.

evolution in high-T_C cuprates (see Ref. 26 and references therein). The zero bias conductance then increases linearly with temperature, a characteristic of the V-shaped background.

It is clear that the spectra in Figs. 3(c) and 3(e) are not BCS-like anymore; a rough estimation yields $\Delta = 1.3$ meV and $\Gamma_{\text{Dynes}} \approx 0.10$ meV. The amplitude of the quasiparticle peaks is further damped with respect to the 2.33-nm case, so that in some areas the peaks disappear completely. The conductance map in Fig. 3(a) allows again visualizing two-scale spatial variations, as observed in the 4- and 2.33-nm samples, with spectral inhomogeneities quite comparable to these latter cases. (i) The zero-bias conductance and the height of quasiparticle peaks vary slightly at the nanometer scale. (ii) The large scale variations appear strikingly to be spatially ordered in parallel bands in some areas of the sample.

Figure 4 illustrates our interpretation of the parallel bands observed in the STS conductance maps [see Fig. 3(a)], when the bias voltage is in the range of the superconducting gap, while a flat surface is seen in the topography. We correlate these

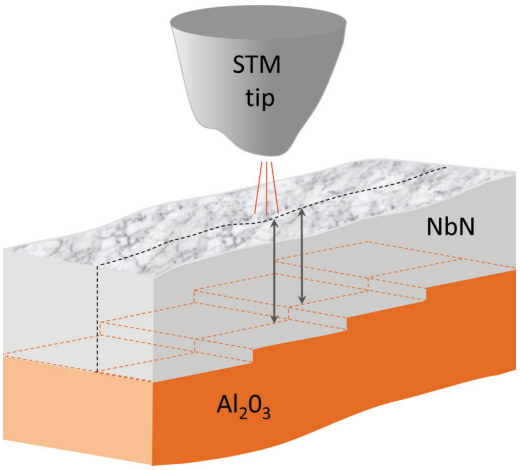

FIG. 4. (Color online) Schematic view of the NbN thin films grown on sapphire substrate measured by STM. The figure emphasizes the fact that from one sapphire atomic terrace to another, the local thickness of the NbN film might slightly vary, leading to sensitive changes of the electronic properties observed in STS conductance maps [see Fig. 3(a)].

parallel bands with 100-nm wide single atomic step variations in the underlying sapphire substrate,[27] resulting in slight thickness fluctuations of the NbN film. This experimental fact should be taken into account in any realistic model describing the SIT but also when designing quantum devices based on SC condensates close to the SIT.

Another astonishing feature is observed: the spectra are dramatically unsensitive to the magnetic field [see Figs. 3(b)–3(d)]; up to $B = 3$ T, no vortices could be observed [see Fig. 3(b)]. However, while bulk H_{C2} is estimated to be $\approx$20 T, H_{C2} decreases with film thickness, but remains larger than 10 T for all studied films and is thus much higher than the fields used here. Vortices are a mesoscopic manifestation of the quantum coherence of the SC condensate, where the phase of the order parameter is spatially well defined and makes 2π turns around each vortex core. Thus it is tempting to interpret this striking result as a break-up of the phase coherence, at least in some regions, in this fragile SC condensate, suggesting a lowered phase stiffness already at $T = 0.4T_C^{\text{bulk}}$, quite before the SIT.

A closer look at Figs. 3(a)–3(d) shows that in magnetic field, the zero-bias conductance homogeneously increases. However, Figs. 3(a) and 3(c) show that in darker (blue) bands small coherence peaks exist, while these are absent in the lighter (green-red) bands. We expect the SC phase coherence to be broken in these latter regions, where the spectral signature is similar to the pseudo-gap-like structure observed in vortex cores. Therefore these "pseudogap" stripes presumably preclude vortices to be observed. We note that the STS spectra in these latter regions resemble the ones calculated on the insulating side of the magnetic field induced SIT,[28] supporting the idea that both systems have in common the loss of SC phase coherence.

C. Effect of magnetic field studied by transport measurement

An important issue concerns the effect of magnetic field on the resistance of the NbN films. In this idea, the square

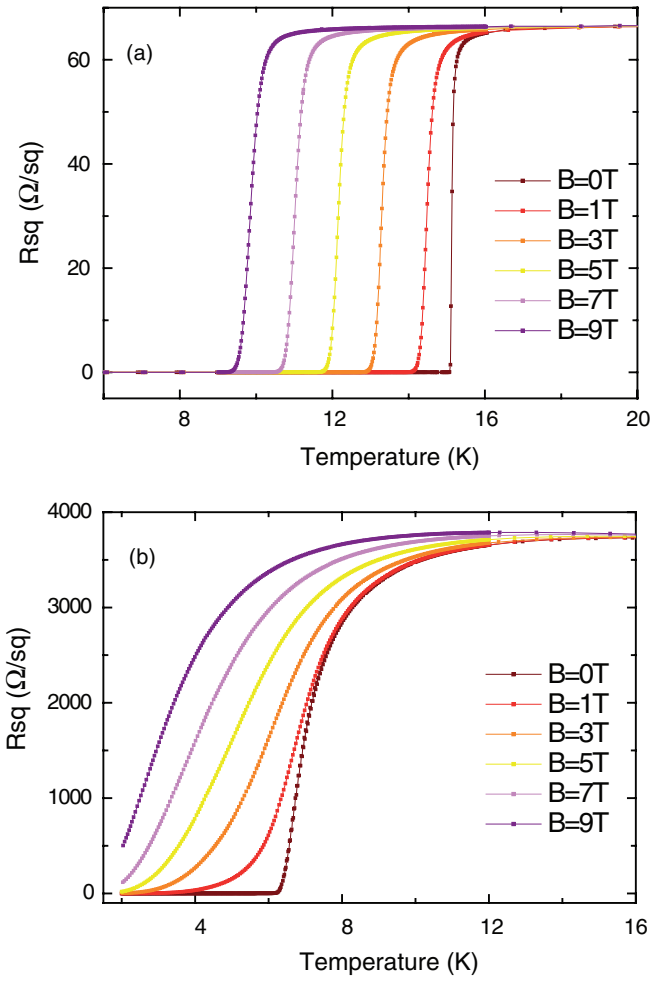

FIG. 5. (Color online) (a) Square resistance vs temperature dependence of a thick 17.5-nm film with $T_C^{17.5\,\text{nm}} = 15$ K, for different magnetic fields in the range 0–9 T. (b) Square resistivity vs temperature dependence of a thin 2.16-nm film with $T_C^{2.16\,\text{nm}} = 6.5$ K for different magnetic fields in the range 0–9 T.

resistance $R_{\text{sq}}(T)$ was measured for a 17.5-nm thick film [see Fig. 5(a)] as well as for a thin 2.16-nm film [see Fig. 5(b)]. It is important to note that the measurement has not been done on the same samples as the one used for tunneling spectroscopic measurement. The thinnest film has a similar thickness and a very close $T_C \approx 6.5$ K, as the one used for tunneling spectroscopic measurement.

At the measurement temperature ($T = 2$ or 4 K), the 17.5-nm-thick film behave very differently than the 2.16-nm film. While the thick 17.5-nm film is fully superconducting at 2 K for all magnetic field in the range 0–9 T, the thinnest film, 2.16 nm, becomes slightly resistive with magnetic field. The value of the square resistance at 2 K (i.e., the measurement temperature) is $\sim$0.03 Ω/sq.

This effect could possibly be attributed to a vortex motion. Indeed, if vortices are moving much faster than the acquisition timescale of a conductance map (several hours), then the conductance would be the result of an average value over the different positions of the moving vortices. In this case, the observed pseudogap inside the vortex core would not reflect the real properties of the vortex core. Note that this

is in agreement with two striking experimental facts. First, as mentioned previously, the presence of a pseudogap at the vortex core. Secondly, the size of the vortex core as observed by STS (∼20 nm) is much larger than the value of the coherence length (⩽5 nm). Both effects can be accounted for by the existence of a vortex motion.

In this scenario, the vortex lattice would become less and less rigid as the film thickness decreases (due to the reduction of vortex-vortex interaction with decreasing thickness), which would give rise to an increase of the vortex motion. This effect would then manifest itself in the resistive behavior of the thinnest films in presence of a magnetic field. In addition, with the reasonable assumption that the timescale of the measurement is much lower that the vortex motion, the STS data would then reflect a time average of the local DOS, explaining both the large vortex size as well as the apparent pseudogap at the vortex core.

IV. DISCUSSION

Let us now discuss our results in view of previous reported works. A hallmark of our tunneling data on approaching the SIT is the development of a more and more pronounced V-shaped background with reducing film thickness. This suggests (see the previous section) enhanced Coulomb effects[31] and is consistent with the fact that T_C versus R_{sq} follows the Finkel'stein law.[7] The observed Δ and T_C progressive reduction (see Table I), with smoothly decreasing $2\Delta_{BCS}/kT_C$ ratio, is consistent with previous reports.[2] Indeed, the reduction follows closely the T_C reduction. This result is also in line with the findings of Chockalingam *et al.*[18] in disordered NbN films, at least for a weak disorder. This effect is in agreement with a scenario where the amplitude of the order parameter is reduced as the SIT transition is approached.[8]

On the other hand, it is in contrast with the results of Sacépé *et al.*,[15] where the ratio $2\Delta/kT_C$ takes higher values and where a clear pseudogap is observed well above T_C. It is probable that increasing further the disorder in our films would also lead to the appearance of a pseudogap well above T_C, and to higher values for $2\Delta/kT_C$.

The evolution of our tunneling spectra with thickness presents as well many surprising similarities with recent studies on thicker NbN films, where the thickness was fixed and the SIT was approached by tuning the disorder (from $k_Fl \sim 10.1$ to 1.2).[18] In particular, thicker NbN films present a T_C versus k_Fl dependence quite comparable to ours, and lead to tunneling characteristics similar to what is reported here. In particular, the features reported for $T_C = 6$ K ($k_Fl = 1.6$) and $T_C = 4.1$ K ($k_Fl = 2.2$) are comparable with those presented for our 2.16 nm film ($T_C = 6.7$ K, $k_Fl \leqslant 2.6$) in terms of (i) a large broadening of the spectra leading to gap filling, (ii) almost vanishing coherence peaks, and (iii) shallow pseudogap above T_C. Regarding (iii), the pseudogap regime might be related to a Berezinskii-Kosterlitz-Thouless transition evidenced recently.[32]

On the other hand, our results are at variance with reports on TiN (3.6–5 nm) and InO films (15 and 30 nm), both suggesting a huge increase of $2\Delta/kT_C$ with increasing disorder.[14,15] The most important difference with respect to TiN and InO samples, is that a very deep pseudogap above T_C was reported, where at T_C, almost all the DOS is depressed at E_F.[14,15] It is important to note that these systems were closer to the SIT ($T_C \leqslant 0.4T_C^{bulk}$). In our case, all $T_C \geqslant 0.4T_C^{bulk}$, and the largest depressed DOS at E_F (films closest to the SIT) is of 35–50%, mostly due to the V-shaped background and not to the pseudogap effect. On the other hand, there are also similarities; observation of small gap inhomogeneities and suppression of the coherence peaks with increasing disorder, while the conductance spectra deviate more and more from BCS behavior.

V. ANALYSIS OF THE RESULTS

Let us now discuss in more details our tunneling data. As mentionned in Sec. II, it is very probable that an oxide layer exists at the surface of the film and it is important to determine in which proportion it could affect the superconducting properties of the film. Our analysis shows that the hypothesis of a proximity layer cannot account for the main features of our tunneling data: the suppression of the quasiparticle peaks at the gap edge and the loss of the superconducting coherence associated with the disappearance of the vortices. This can be shown by calculating the effect of a proximity layer, as described in the following section.

A. Does the passivation layer induce a proximity effect?

The proximity effect in the DOS can be taken into account by the McMillan model[29] (or equivalently, by the Usadel-bilayer model in the limit where $d < \xi$, d being the typical thickness of the proximity layer, since these two formalisms are mathematically equivalent[30]). Applying this model to the thick samples (15 and 8 nm) leads to the conclusion that the hypothetical proximity layer is very strongly coupled to the superconducting layer (high quasiparticle scattering Γ_N from the proximity layer to the SC layer in the McMillan formalism[29] or, equivalently, high boundary transparency in Usadel formalism).

Indeed, let us consider the case of a non-SC proximity layer (i.e., with zero SC gap) coupled to a superconductor with an intrinsic gap of $\Delta_{NbN} = 2.9$ meV. We first consider the case of a NbN film much thicker than the oxide layer. We assume a ratio of 20 between the integrated density of states $\frac{N_S d_S}{N_N d_N} \sim 20$, where d_S, d_N, N_S, and N_N are respectively the thickness and the density of states by unit volume in the SC layer and in the normal layer.

The first simulation [see Fig. 5(a)] is obtained with a coupling parameter $\Gamma_N = 1$ meV. The blue curves in Fig. 6 correspond to the density of states in the proximity layer and the black curves correspond to the density of states in the superconducting layer. The red curves are the simulated differential tunneling conductance measured by STM on-top of the proximity layer at low temperature ($T = 2.3$ K). The quasiparticle coupling between the SC and the normal layer gives rise to a very small induced gap in the proximity layer. It is clearly different from what is observed in the experiment [see Fig. 1(c) for the 15-nm film], and thus rules out the hypothesis of a weak coupling.

Next, we consider a larger coupling, $\Gamma_N = 10$ meV. As can be seen in Fig. 5(b), the resulting excitation spectrum exhibits a strong departure from BCS. For a very strong coupling,

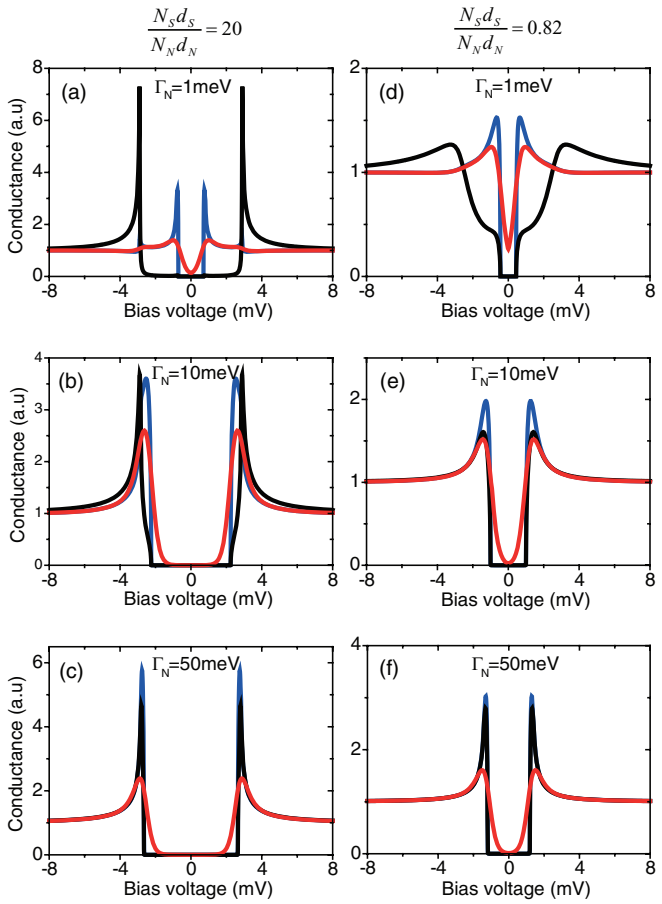

FIG. 6. (Color online) Superconducting layer coupled to a normal layer in the framework of the McMillan model[29] for different values of the coupling parameter $\Gamma_N = 1$, 10, and 50 meV, and assuming a ratio of 20 (a)–(c) and 0.82 (d)–(f) between the integrated density of states $\frac{N_S d_S}{N_N d_N} \approx 20$, where N_S and N_N are the density of states by unit volume in the superconducting and normal layers, respectively. Black: partial DOS in the superconducting layer. Blue: partial DOS in the proximity layer. Red: simulated tunneling conductance at $T = 2.3$ K.

$\Gamma_N = 50$ meV $\gg \Delta_{\mathrm{NbN}}$ [see Fig. 5(c)], we recover a BCS-like density of state in the proximity layer. This form of the tunneling DOS is compatible with our observations [see Fig. 1(c)].

Let us now consider the situation in the thinnest superconducting sample with a thickness $d = 2.16$ nm. We assume a strong coupling between the superconductor and the proximity layer. In this sample, T_C is divided by 2.2 as compared to the thickest samples. Such a T_C reduction means, in the strong coupling approximation, that the ratio $\frac{N_S d_S}{N_N d_N}$ should be of the order or less than unity ($\sim$0.82). The three simulations in Figs. 6(d)–6(f) are done for the following Γ_N values: 1 [see Fig. 5(d)], 10 [see Fig. 5(e)], and 50 meV [see Fig. 5(f)] as previously, and assuming a ratio of 0.82 between the integrated density of states of both layers. It is remarkable that the quasiparticle peaks in the tunneling spectra remain extremely robust, in complete contradiction with our experimental data.

Moreover, a T_C reduction of a factor of 2.2 would imply a contribution of 55% from the DOS of the proximity layer which is $\sim$0.5 to 1 nm thick. This is not very likely since, as the samples were exposed to air, the top-layer should share some common properties with the ones of the maximally oxidized form of Nb (Nb_2O_5), which is nominally an insulator and not a metal. Even if we assume that the passivation layer is metallic, we do not expect its DOS at the Fermi Level to be of the order of the one of the underlying NbN layer. Indeed, consider the case of an integrated DOS ratio of 0.82, a 1-nm-thick oxide layer and 1.16-nm-thick layer of NbN. It would then lead to a $N_N = 1.4N_S$, and for a 0.5-nm oxide layer, we find $N_N = 4N_S$. This would imply that a strongly disordered oxide has a much higher density of states at the Fermi level than a good metal, which is clearly not reasonable. Thus, it is improbable that the T_C reduction can be imputed solely to a hypothetical proximity layer.

Concerning more specifically the V-shaped background observed in the experiment, it follows from the simulations that it cannot be explained in terms of a proximity scenario. In summary, our analysis shows that a proximity effect cannot account for the shape of the measured tunneling spectra in our NbN films.

B. Dependence of the critical temperature with film thickness: Effect of Coulomb interactions

The analysis of the T_C dependence as a function of film thickness can give a precious information about the physical mechanisms involved as the film reaches the 2D limit. We analyzed the dependence of the critical temperature T_C of the films as a function of their sheet resistance $R_{\mathrm{sq}}(T)$. Figure 7 shows that the dependence is quite linear in this range of resistances and follows almost perfectly the Finkel'stein's law.[7] This suggests that the joint action of Coulomb interactions and scattering by the disorder (grain boundaries, impurities, surface and interface boundaries) are quite efficient mechanisms to reduce the critical temperature on the metallic side of the SIT, and thus to reduce also the gap amplitude. The fact that the Finkel'stein's model describes well the T_C reduction is consistent with the appearence of a large V-shaped background that develops in the tunneling conductance dI/dV, and superposes to the SC gap. Indeed,

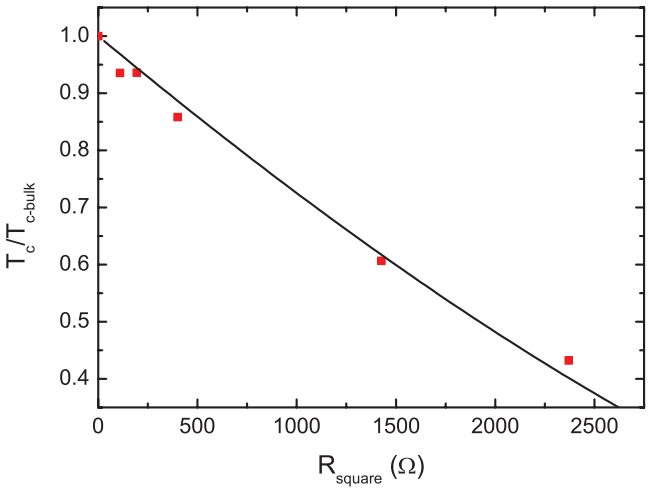

FIG. 7. (Color online) Dependence of $T_C/T_{C\text{-bulk}}$, the superconducting critical temperature normalized by the bulk one, as a function of their square resistance R_{sq} in the normal state at 40 K, for ultrathin NbN films. Squares: experimental data extracted from resistivity measurements; continuous line: fit by the Finkel'stein model (see text).

enhanced Coulomb interactions with increasing disorder are known to reduce the tunneling DOS at E_F,[31] and from our spectra we clearly see the V-shaped background to become deeper as T_C is reduced for the thinnest films. Furthermore, keeping the original notation of Finkel'stein, $1/\Gamma = \ln(\tau T_{C0}) = -5.65$ in our case, which attests that strong disorder/Coulomb interactions exist in our films, as $|\ln(\tau T_{C0})| \gg 1$. The comparison with the values obtained for TiN $(-6.2; -6.8)$[14] or MoGe (-7)[4] shows that NbN films undergo comparably strong disorder-enhanced Coulomb interactions, the exact $\ln(\tau T_{C0}) = -5.65$ value indicating that these effects are a bit smaller in NbN than in TiN or MoGe.

C. Zero-bias tunneling conductance

It is noticeable that, as the film thickness is reduced, the zero bias conductance increases at low temperature (2.3 K). It is important to note that this is a real effect that cannot be attributed to a thermal smearing. The simulated BCS spectrum shown in Fig. 3(e) suggests an energy gap value of 1.3 meV. At the temperature of 2.3 K with a T_C of 6.7 K (which is almost $\sim T_C/3$), the expected BCS spectrum would lead to almost zero conductance at $V = 0$. This clearly does not correspond to the measured spectra. Thus, in a BCS scenario, there should exist an additional intrinsic pair-breaking mechanism that would populate electronic states inside the gap region, leading to a nonzero DOS. In the spirit of the Finkel'stein's model, this could be accounted for by following Ebisawa *et al.*,[6] who calculated the pair breaking parameter in a two-dimensional dirty superconductor. In the shown simulated spectrum [blue one in Fig. 3(e)], we estimated this effect using the spectral broadening parameter[24] Γ_{Dynes} leading to a value of $\sim$0.10 meV. On the other hand for the 2.33-, 4-, and 8-nm films the Γ_{Dynes} values of the simulated BCS spectra are, respectively, 0.05, 0.01, and 0.01 meV, while the 15 nm could be simulated at about 2.3 K without any Γ_{Dynes} parameter. The values we have used for Γ_{Dynes} are quite in agreement with the tunneling data of Chockalingam *et al.*[18] where at 2.2 K for (a) $T_C = 7.7$ K, $k_F l \sim 1.4$, $\Gamma_{\text{Dynes}} = 0.08$ meV; (b) $T_C = 9.5$ K, $k_F l \sim 2.3$, $\Gamma_D = 0.07$ meV; and (c) $T_C = 14.9$ K, $k_F l \sim 6$, $\Gamma_{\text{Dynes}} = 0.006$ meV. This reinforces similarities between our results on ultrathin NbN films and the previous results obtained on 50-nm-thick film where the SIT was approached by tuning disorder.

VI. CONCLUSION

In conclusion, the tunneling conductance of NbN thin films exhibits unconventional signatures as the film thickness approaches the 2D limit. Clear deviations from the prediction of the BCS theory are observed as the film thickness is reduced and $k_F l$ lowers, such as the decrease of the coherence peaks, spatial inhomogeneities, and a V-shaped spectral background, which becomes more and more pronounced when approaching the SIT.

Analysis of the results shows that in NbN ultrathin films approaching SIT, Coulomb interactions are an efficient mechanism to reduce the SC gap and T_C, and are well-described by the Finkel'stein model.[7] In addition, the ratio of $2\Delta/kT_C$ remains roughly constant as a function of the film thickness, which is also in agreement with a scenario where the amplitude of the order parameter is reduced as the SIT transition is approached.[8]

However, the thinnest SC films exhibits some deviations from this scenario. The shape of the spectrum cannot be described by the BCS DOS. Already at $T_C \approx 0.4 T_C^{\text{bulk}}$, the coherence peaks almost vanish and the vortex lattice disappear. Both effects suggest a weakening of the phase coherence in the thinnest films. This in qualitative agreement, at least for a low disorder, with several numerical works where the interplay between superconductivity and localization with disorder was studied.[10–13] It might indicate a crossover from a fermionic scenario toward a bosonic scenario with pair localization as observed by Sacépé *et al.*[15] Further investigations very close to the SIT are necessary to clarify the role and the nature the V-shaped background.

ACKNOWLEDGMENTS

The authors acknowledge fruitful discussions with B. Sacépé and C. Chapelier. The work is supported in part by the UPMC émergence project-contract 11-272 and by the DFG Center for Functional Nanostructures under subproject A4.3.

[1] V. F. Gantmakher and V. T. Dolgopolov, Physics - Uspekhi **53**, 1 (2010).
[2] Allen M. Goldman and Nina Marković, Phys. Today **51**, 39 (1998).
[3] B. G. Orr, H. M. Jaeger, and A. M. Goldman, Phys. Rev. B **32**, 7586 (1985); A. E. White, R. C. Dynes, and J. P. Garno, *ibid.* **33**, 3549 (1986).
[4] J. M. Graybeal and M. R. Beasley, Phys. Rev. B **29**, 4167 (1984); R. C. Dynes, A. E. White, J. M. Graybeal, and J. P. Garno, Phys. Rev. Lett. **57**, 2195 (1986).
[5] J. M. Valles, Jr., R. C. Dynes, and J. P. Garno, Phys. Rev. Lett. **69**, 3567 (1992).
[6] H. Ebisawa, S. Maekawa, and H. Fukuyama, Solid State Commun. **45**, 75 (1983).
[7] A. M. Finkel'shtein, Pis'ma ZhETF **45**, 37 (1987) [JETP Letters **45**, 46 (1987)].
[8] A. M. Finkel'stein, Physica B **197**, 636 (1994).
[9] M. V. Feigel'man, L. B. Ioffe, V. E. Kravtsov, Ann. Phys. **325**, 1390 (2010).
[10] C. Huscroft and R. T. Scalettar, Phys. Rev. Lett. **81**, 2775 (1998).
[11] A. Ghosal, M. Randeria, and N. Trivedi, Phys. Rev. Lett. **81**, 3940 (1998); Phys. Rev. B **65**, 014501 (2001).
[12] K. Bouadim, Y. L. Loh, M. Randeria, and N. Trivedi, Nat. Phys. **7**, 884 (2011).
[13] G. Seibold, L. Benfatto, C. Castellani, and J. Lorenzana, Phys. Rev. Lett. **108**, 207004 (2012).
[14] B. Sacepe, C. Chapelier, T. I. Baturina, V. M. Vinokur, M. R. Baklanov, and M. Sanquer, Phys. Rev. Lett. **101**, 157006 (2008); B. Sacépé *et al.*, Nat. Comm. **1** (2010).
[15] B. Sacépé *et al.*, Nat. Phys. **7**, 239 (2011).
[16] G. N. Gol'tsman *et al.*, Appl. Phys. Lett. **79**, 705 (2001).

[17]M. Hofherr *et al.*, J. Appl. Phys. **108**, 014507 (2010).
[18]S. P. Chockalingam, M. Chand, J. Jesudasan, V. Tripathi, and P. Raychaudhuri, Phys. Rev. B **77**, 214503 (2008); S. P. Chockalingam, M. Chand, A. Kamlapure, J. Jesudasan, A. Mishra, V. Tripathi, and P. Raychaudhuri, *ibid.* **79**, 094509 (2009); M. Mondal, A. Kamlapure, M. Chand, G. Saraswat, S. Kumar, J. Jesudasan, L. Benfatto, V. Tripathi, and P. Raychaudhuri, Phys. Rev. Lett. **106**, 047001 (2011).
[19]A. Semenov *et al.*, Phys. Rev. B **80**, 054510 (2009).
[20]We cannot exclude weak variations of the nanocrystallite structure with thickness.
[21]J. R. Kirtley, S. I. Raider, R. M. Feenstra, and A. P. Fein, Appl. Phys. Lett. **50**, 1607 (1987).
[22]S. Kashiwaya, M. Koyanagi, A. Shoji, M. Matsuda, and H. Shibata, Physica B **169**, 465 (1991).
[23]G. J. C. van Baarle, A. M. Troianovski, T. Nishizaki, P. H. Kes, and J. Aarts, Appl. Phys. Lett. **82**, 1081 (2003).
[24]R. C. Dynes, V. Narayanamurti, and J. P. Garno, Phys. Rev. Lett. **41**, 1509 (1978).
[25]T. Cren, D. Roditchev, W. Sacks, and J. Klein, Europhys. Lett. **54**, 84 (2001); Y. H. Kim, R. Yu, S. P. Kulik, Y. Shih, and M. O. Scully, Phys. Rev. Lett. **84**, 1 (2000).
[26]O. Fischer, M. Kugler, I. Maggio-Aprile, C. Berthod, and C. Renner, Rev. Mod. Phys. **79**, 353 (2007).
[27]M. Yoshimoto, T. Maeda, T. Ohnishi, H. Koinuma, O. Ishiyama, M. Shinohara, M. Kubo, R. Miura, and A. Miyamoto, Appl. Phys. Lett. **67**, 2615 (1995).
[28]Y. Dubi, Y. Meir, and Y. Avishai, Nature (London) **449**, 876 (2007).
[29]W. L. McMillan, Phys. Rev. **175**, 537 (1968).
[30]A. A. Golubov, E. P. Houwman, J. G. Gijsbertsen, V. M. Krasnov, J. Flokstra, H. Rogalla, M. Yu. Kupriyanov, Phys. Rev. B **51**, 1073 (1995).
[31]B. L. Altshuler, A. G. Aronov, and P. A. Lee, Phys. Rev. Lett. **44**, 1288 (1980).
[32]M. Mondal, S. Kumar, M. Chand, A. Kamlapure, G. Saraswat, G. Seibold, L. Benfatto, and P. Raychaudhuri, Phys. Rev. Lett. **107**, 217003 (2011).